8th International Symposium on
Advanced Electromechanical Motion Systems

ELECTROMOTION 2009
EPE Chapter “Electric Drives”
Joint Symposium
July 1 – 3, 2009, Lille - France

PROCEEDINGS

To access any article: go to the next page, click on the session and then on the title.

PS1: ‘*Decoupled generation providing quality power’*

PS2: ‘*Real-Time Simulation of Variable Speed Drives’*

OS1: *‘Design and analysis of permanent-magnet motors’*

OS2 / Special Session: *‘Renewable energies for electricity production I’*

OS3: *‘Modeling and power management in electric transport systems’*

OS4: *‘Performance analysis and improvement of AC motors’*

OS5 / Special Session: *‘Fuel cell systems: modeling, control and design’*

OS6: *‘Power supply and motion control of industrial drives’*

OS7: *‘Electric vehicle and traction drives’*

OS8 / Special Session: *‘Energy management and power control of hybrid power systems’*

OS9: ‘*Control of permanent-magnet synchronous motor drives*’

OS10 / Special Session: *‘Renewable energies for electricity production II’*

OS11: *‘Novel actuators and microelectromechanical systems’*

OS12: *‘Distributed energy generation systems’*

DS1: *‘Design and analysis of electromagnetic devices’*

DS2: *‘Advanced control of power converters and motor drives’*

Analysis of Torsional Oscillation of the Drive Train in Horizontal-Axis Wind Turbine

M.Todorov[1], I. Dobrev[2] and F. Massouh[2]
[1]Department of Aeronautics, Technical University of Sofia, Sofia, Bulgaria
[2]Laboratory of Fluid Mechanics, ENSAM, Paris, France

Abstract **- The unsteadiness of rotor inflow caused by the atmosphere creates continuous variations of blade loads and rotor torque. Usually these loads are amplified by rotor shaft and gearbox elasticity and inertia. The authors propose here a dynamic multi-body model where the wind turbine includes a rotor, a drive train and an electrical generator. The drive train has a three stage gearbox which contains two high-speed parallel gear stages and a low-speed planetary gear stage. The model consists of 10 bodies and has 8 degrees of freedom taking into account the stiffness of the engaged tooth pairs. In this model the aerodynamic torque is applied as an external load. The calculation permits to obtain natural frequencies, mode shapes, time series of torsional oscillations and amplitude-frequency characteristics for an industrial wind turbine. The results show that transient loads in the gearbox are very high and need special attention.**

I. INTRODUCTION

The wind energy application has been growing rapidly for the last few years. From 1995 to 2006 the global installed capacity of wind energy increased 20 times. This trend is expected to continue in Europe. The increase in the rotor size and hence the turbine size leads to complicated design of drive train in the wind turbine besides higher requirements of turbine reliability.

Design calculations for wind turbine base on simulation of mechanical loads on the turbine components caused by external forces. The external forces are the wind, the electricity grid and sea waves for offshore applications.

The multi-body simulation techniques are used to analyze the loads on internal components of drive trains. The simplest model with one degree of freedom (DOF) per drive train component is used to investigate only torsional vibrations in the drive train. In this model all bodies have one DOF, i.e. the rotation around their axis of symmetry. Therefore the coupling of two bodies involves 2 DOF's. Gear contact forces between two wheels are modeled with linear spring acting in the plane of action along the contact line (normal to the tooth surface). This modeling is valid for heavily to moderately loaded gears [4, 21]. More complex model with 6 DOF's per drive train component is used for investigation of the influence of bearing stiffness on the internal dynamics of the drive train. All drive train components are treated as rigid bodies. The linkages in the multi-body model, representing the bearing and tooth flexibilities have 12 DOF's [28, 46]. Finally, a flexible model in which the drive train components are modeled as finite element models instead of rigid bodies is used [6, 8, 26, 47]. This model adds a possibility of calculating stress and deformation in the drive train components continuously with time. Every addition to the model leads to additional information about dynamics of the drive train but makes the modeling and the simulation more complicated. References [25, 28, 50, 51] present the effects of the tooth defects and the wear on the gear dynamics.

The applications of these modeling techniques on different drive trains of wind turbines are presented in [14, 18, 19, 29-32, 34, 36, 39-41, 42, 43, 45, 48]. The dynamic characteristics of asynchronous and synchronous machines are presented in detail in [1, 2, 20, 22]. Different simulations for specific wind turbines are presented in [12, 13, 17, 35, 38, 42-44].

II. DYNAMIC MODEL OF WIND TURBINE

The wind turbine consists of a rotor, a drive train and a generator (Fig.1). The drive train has a gearbox with three stages. The gear stages include two high-speed parallel gear stages (spur gear pairs) and a low-speed planetary gear stage (three identical planets with spur teeth, sun and fixed ring wheel) (Fig.2). The dynamic multi-body model is shown in Fig.3. It consists of a rotor with 3 rigid blades, a low-speed elastic shaft, a gearbox with 3 gear stages, a high-speed elastic shaft and a generator rotor. Thus the model consists of 10 bodies and 8 DOF's.

The gear contact forces between wheels are modeled by linear spring acting in the plane of action along the contact line (normal to the tooth surface) [2-4, 52]. The stiffness gear is defined as the normal distributed tooth force in the normal plane causing the deformation of one or more engaging tooth pairs, over a distance of 1 μm, normal to the evolvent profile

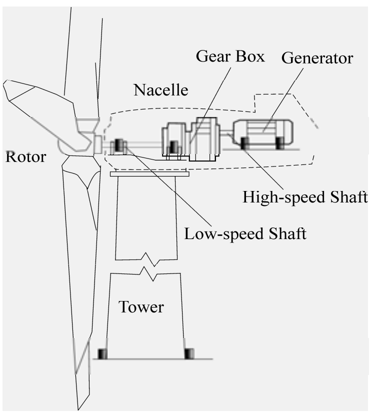

Figure 1. Schematic sketch of wind turbine

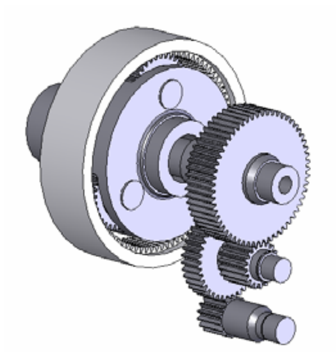

Figure 2. Gearbox

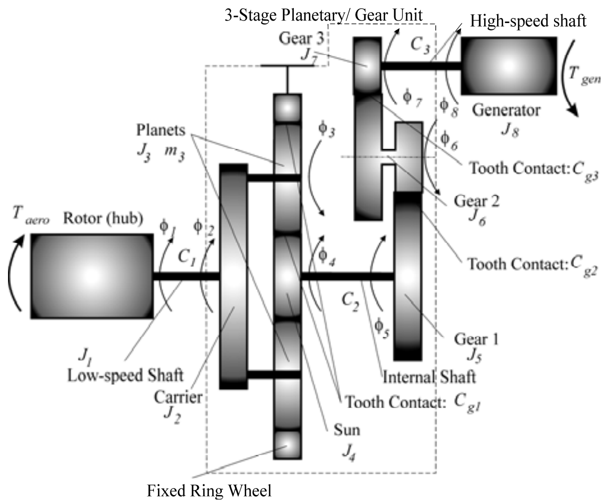

Figure 3. Dynamical model of wind turbine

in the normal plane [11]. This deformation results from the bending of the teeth in contact between the two gear wheels, of which one is fixed and the other is loaded. Damping and friction forces are not included. These assumptions are valid for heavily to moderately loaded gears [4, 21].

In this article Lagrange's equations are used to obtain the equations of the torsional vibrations of wind turbine [2, 7, 10, 27, 37, 49]. The vector of the generalized co-ordinates is

$$\{\phi\} = \begin{bmatrix} \phi_1 & \phi_2 & \phi_3 & \phi_4 & \phi_5 & \phi_6 & \phi_7 & \phi_8 \end{bmatrix}^T \tag{1}$$

where ϕ_i (i=1-8) are the absolute rotational angles of the rotor (hub), carrier, planets, sun, gear 1, gear 2, gear 3 and generator rotor (Fig. 3).

The differential equations describing the torsional vibrations of the wind turbine are

$$[J]\{\ddot{\phi}\} + [C]\{\phi\} = \{T\} \tag{2}$$

The matrices J and C describe the linear properties of mass inertia and stiffness. Their numbers are

$$[J] = diag\begin{bmatrix} J_1 & J_2 + 3m_3 r_{C1}^2 & 3J_3 & J_4 & J_5 & J_6 & J_7 & J_8 \end{bmatrix}$$

$$[C] = \begin{bmatrix} C_1 & -C_1 & 0 & 0 & 0 & 0 & 0 & 0 \\ -C_1 & \begin{matrix} C_1 + \\ +6C_{g1}r_{c1}^2 \end{matrix} & 0 & -3C_{g1}r_{C1}r_4 & 0 & 0 & 0 & 0 \\ 0 & 0 & 6C_{g1}r_3^2 & 0 & 0 & 0 & 0 & 0 \\ 0 & -3C_{g1}r_{C1}r_4 & 0 & 3C_{g1}r_4^2 + C_2 & -C_2 & 0 & 0 & 0 \\ 0 & 0 & 0 & -C_2 & \begin{matrix} C_2 + \\ +C_{g2}r_5^2 \end{matrix} & C_{g2}r_5 r_{61} & 0 & 0 \\ 0 & 0 & 0 & 0 & C_{g2}r_5 r_{61} & \begin{matrix} C_{g2}r_{61}^2 + \\ +C_{g3}r_{62}^2 \end{matrix} & C_{g3}r_{62}r_7 & 0 \\ 0 & 0 & 0 & 0 & 0 & C_{g3}r_{62}r_7 & \begin{matrix} Cg_3 r_7^2 + \\ +C_3 \end{matrix} & -C_3 \\ 0 & 0 & 0 & 0 & 0 & 0 & -C_3 & C_3 \end{bmatrix}$$

The vector of the external forces caused by the wind and the electricity grid is

$$\{T\} = \begin{bmatrix} T_{aero} & 0 & 0 & 0 & 0 & 0 & 0 & T_{gen} \end{bmatrix}^T \tag{3}$$

where T_{aero} and T_{gen} are the aerodynamic and electromagnetic torques.

III. AERODYNAMIC TORQUE

Different methods can be used to calculate the aerodynamic forces acting on the blades of a wind turbine. The most advanced ones are numerical methods solving the Navier-Stokes equations for the compressible flow as well as the flow near the blades. The method that is used is based on the blade element momentum theory [9, 16, 24]. This method gives good accuracy with respect to time cost. In this method, the turbine blades are divided into a number of independent elements along the length of the blade (Fig. 4). At each section, a force balance is applied involving 2D section lift L and drag D with the thrust P and torque T_{aero} produced by the section. The axial and angular momentum is also balanced. The set of non-linear equations are produced which can be solved numerically for each blade section [5, 9].

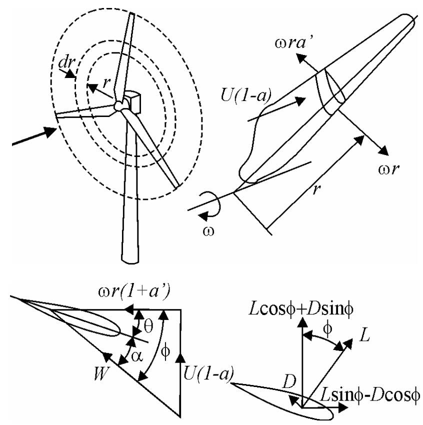

Figure 4. Blade element velocities and forces [9]

The lift force L per unit length is perpendicular to the relative speed W of the wing:

$$L = \frac{\rho c(r)}{2} W^2 C_L \tag{4}$$

where $c(r)$ is the blade chord length. The drag force D per unit length, which is parallel to W is

$$D = \frac{\rho c(r)}{2} W^2 C_D \tag{5}$$

Since the forces normal and tangential to the rotor plane are interested, the lift L and drag D are projected on these directions (Fig. 4)

$$F_N = L\cos\phi + D\sin\phi \tag{6}$$
$$F_T = L\sin\phi - D\cos\phi \tag{7}$$

The information about the lift and drag airfoil coefficients C_L and C_D is required. These coefficients are given as functions of the angle of attack

$$\alpha = \phi - \theta \tag{8}$$

If the angle of attack α exceeds about 15° the blade will stall. This means that the boundary layer on the upper surface becomes turbulent, and the drag will increase and the lift will decrease.

The flow angle is

$$\tan\phi = \frac{(1-a)U_\infty}{(1+a')\omega r} \tag{9}$$

The lift and drag coefficients C_L and C_D are projected onto the normal and tangential directions

$$C_N = C_L\cos\phi + C_D\sin\phi \tag{10}$$
$$C_T = C_L\sin\phi - C_D\cos\phi \tag{11}$$

The solidity σ is defined as the fraction of the annular area in the control volume, which is covered by the blades

$$\sigma(r) = \frac{c(r)N}{2\pi r} \tag{12}$$

where N is the number of blades.

The normal force and the torque per unit length on the control volume of thickness dr are

$$dP = NF_N dr = \frac{1}{2}\rho N \frac{U_\infty^2(1-a)^2}{\sin^2\phi} cC_N dr \tag{13}$$

$$dT_{aero} = rNF_T dr = \frac{\rho N}{2}\frac{U_\infty(1-a)\omega r^2(1+a')}{\sin\phi\cos\phi} cC_T dr \tag{14}$$

The induction factors are defined as

$$a = \frac{1}{\dfrac{4\sin^2\phi}{\sigma C_N}+1} \tag{15}$$

$$a' = \frac{1}{\dfrac{4\sin\phi\cos\phi}{\sigma C_T}-1} \tag{16}$$

For each control volume the following algorithm is applied:

1. Initially put $a = a' = 0$.
2. Compute ϕ using (11).
3. Compute α using (10).
4. Read C_L and C_D from airfoil data table.
5. Compute C_N and C_T from (12) and (13).
6. Calculate new a and a' from (17) and (18).
7. If a and a' has changed more than a certain tolerance, go to 2 or else finish.
8. Compute the local forces on the segments of the blades.

IV. Electromagnetic torque of generator

The voltage equations for the induction machine in a d-q synchronous reference frame can be written in complex form with the real axis d and the imaginary axis q according to Kovacs [22]

$$u_s = R_s i_s + \dot{\psi}_s + j\omega_e\psi_s \tag{17}$$
$$u_r = R_r i_r + \dot{\psi}_r + j(\omega_e - \omega_r)\psi_r \tag{18}$$

where i_s and i_r are the currents, ψ_s and ψ_r are the fluxes, R_s and R_r are the resistances of the stator and the rotor. The synchronous speed is $\omega_e = 2\pi f_{net}$, where f_{net} is the grid frequency. The electrical rotor speed is $\omega_r = p\Omega_r$, where p is the pole pairs, and Ω_r is the mechanical speed of generator rotor. The complex operator is $j = \sqrt{-1}$.

The relationship between current and flux is

$$\begin{Bmatrix} i_s \\ i_r \end{Bmatrix} = \frac{1}{D}\begin{bmatrix} L_{rr} & -L_m \\ -L_m & L_{ss} \end{bmatrix}\begin{Bmatrix} \psi_s \\ \psi_r \end{Bmatrix} \tag{19}$$

where $L_m = \dfrac{X_m}{\omega_e}$, $L_{ss} = \dfrac{X_m + X_s}{\omega_e}$, $L_{rr} = \dfrac{X_m + X_r}{\omega_e}$, $D = L_{ss}L_{rr} - L_m^2$ and X_m is the magnetizing reactance, X_r and X_s are the leakage reactances of the rotor and the stator. By inserting the equation of current (19) into (17) and (18) the electro-magnetic fluxes are obtained as

$$\begin{Bmatrix} \dot{\psi}_s \\ \dot{\psi}_r \end{Bmatrix} = \begin{bmatrix} -\dfrac{R_s L_{rr}}{D} - j\omega_e & \dfrac{R_s L_m}{D} \\ \dfrac{R_r L_m}{D} & -\dfrac{R_r L_{ss}}{D} - j(\omega_e - \omega_r) \end{bmatrix}\begin{Bmatrix} \psi_s \\ \psi_r \end{Bmatrix} + \begin{Bmatrix} u_s \\ u_r \end{Bmatrix} \tag{20}$$

The electromagnetic generator torque is calculated as

$$T_{gen} = \frac{3pL_m}{2D}\operatorname{Im}\{\psi_s \overline{\psi}_r\} \tag{21}$$

where $\overline{\psi}_r$ is the complex conjugate of ψ_r. To avoid numerical instability (20) is modified. Thomsen in [44] assumes that the stator flux is almost constant ($\dot{\psi}_s \equiv 0$). Equations (20) is rewritten to one complex differential equation describing the flux of rotor

$$\dot{\psi}_r = \left[\frac{R_r R_s L_m^2}{D^2\left(\frac{R_s L_{rr}}{D} + j\omega_e\right)} - \frac{R_r L_{ss}}{D} - j(\omega_e - \omega_r) \right]\psi_r + + \frac{R_r L_m}{D\left(\frac{R_s L_{rr}}{D} + j\omega_e\right)} u_s + u_r \quad (22)$$

and one complex equation describing the flux of stator

$$\psi_s = \frac{R_s L_m}{D\left(\frac{R_s L_{rr}}{D} + j\omega_e\right)}\psi_r + \frac{u_s}{\frac{R_s L_{rr}}{D} + j\omega_e} \quad (23)$$

V. RESULTS

The rotor characteristics are listed in Table I, the drive train data are listed in Table II, and the generator data are listed in Table III.

The natural frequencies and mode shapes are obtained by equation (6)

$$\left([J]^{-1}[C] - \lambda[E]\right)\{\varphi\} = 0 \quad (24)$$

All calculations are accomplished using the codes of MATLAB. The natural frequencies in Hz are

716.19 435.30 290.74 249.40 187.46 66.52 2.51 0.27

The mode shapes are shown in Fig.5.

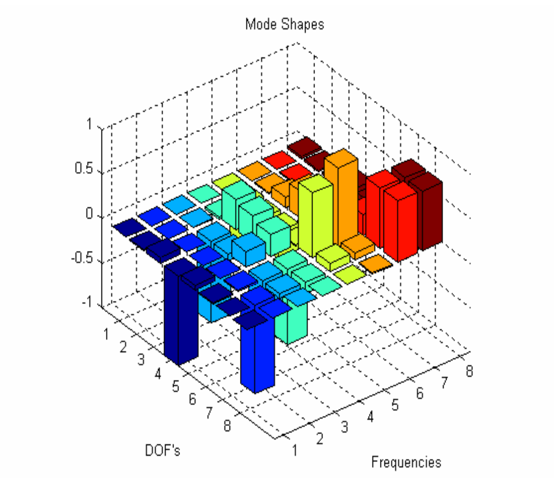

Figure 5. Mode shapes of wind turbine

TABLE I. ROTOR CHARACTERISTICS

N -number of blades	3
D -rotor diameter (m)	56
Blade airfoil NACA 4412	
c_r -root chord (m)	3.3
c_t -tip chord (m)	0.9
ω -rotational speed (rpm)	18
θ -pitch angle (°)	2
β -linear twist of blade (°)	10
W -wind speed (m/s)	6

TABLE II. DRIVE TRAIN DATA

J_1 -inertia of the rotor (kg·m^2)	$4.18\cdot10^6$
J_2 -inertia of the carrier (kg·m^2)	57.72
m_3 -mass of the planet (kg)	57.79
J_3 -inertia of the planet (kg·m^2)	1.12
J_4 -inertia of the sun (kg·m^2)	0.86
J_5 -inertia of the gear 1 (kg·m^2)	14.32
J_6 -inertia of the gear 2 (kg·m^2)	1.62
J_7 -inertia of the gear 3 (kg·m^2)	0.20
J_8 -inertia of the generator (kg·m^2)	93.22
C_1 -stiffness of the low-speed shaft (Nm/rad)	$7.19\cdot10^7$
C_2 -stiffness of the internal shaft (Nm/rad)	$1.40\cdot10^7$
C_3 -stiffness of the high-speed shaft (Nm/rad)	$0.15\cdot10^7$
C_{g1} -stiffness of the engaging tooth pairs in the low-speed planetary gear stage (N/m)	$0.73\cdot10^8$
C_{g2} -stiffness of the engaging tooth pairs in the 1st high-speed parallel gear stage (N/m)	$2.02\cdot10^9$
C_{g3} - stiffness of the engaging tooth pairs in the 2nd high-speed parallel gear stage (N/m)	$0.11\cdot10^8$
r_{C1} - carrier radius (mm)	270
r_3 - planet radius (mm)	160
r_4 - sun radius (mm)	110
r_5 - radius of gear 1 (mm)	290
r_{61} - radius of gear 2 from the 2nd stage (mm)	95
r_{62} - radius of gear 2 from the 3rd stage (mm)	185
r_7 - radius of gear 3 (mm)	80
α - pressure angle (°)	20
gear ratio	34.654

TABLE III. THREE-PHASE ASYNCHRONOUS GENERATOR DATA

R_s -stator resistance (Ω)	0.001164
R_r -rotor resistance (Ω)	0.00131
X_m -magnetizing reactance (Ω)	0.941
X_r -rotor leakage reactance (Ω)	0.0237
X_s -stator leakage reactance (Ω)	0.022
U -voltage (V)	380
f_{net} -grid freq (Hz)	50
p -poles	2 pairs

The results of time simulation are shown in Fig.6. The amplitude-frequency characteristics are shown in Fig.7.

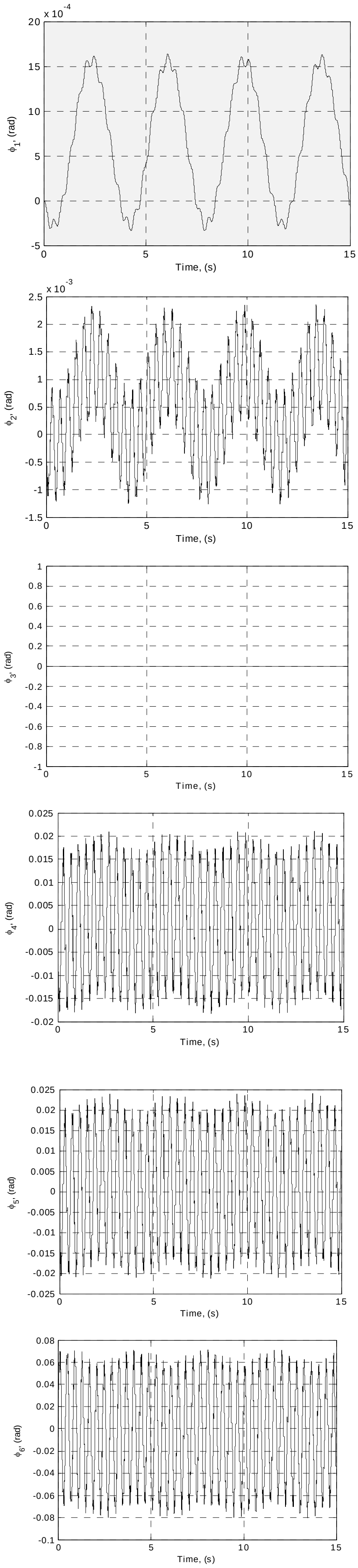

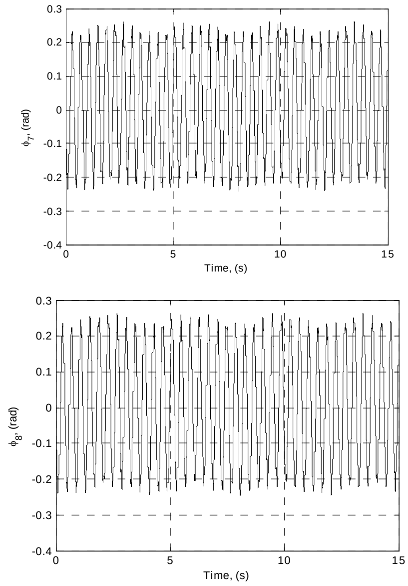

Fig. 6. Rotational angles. From top: Rotor (hub), carrier, planets, sun, gear 1, gear 2, gear 3, generator rotor

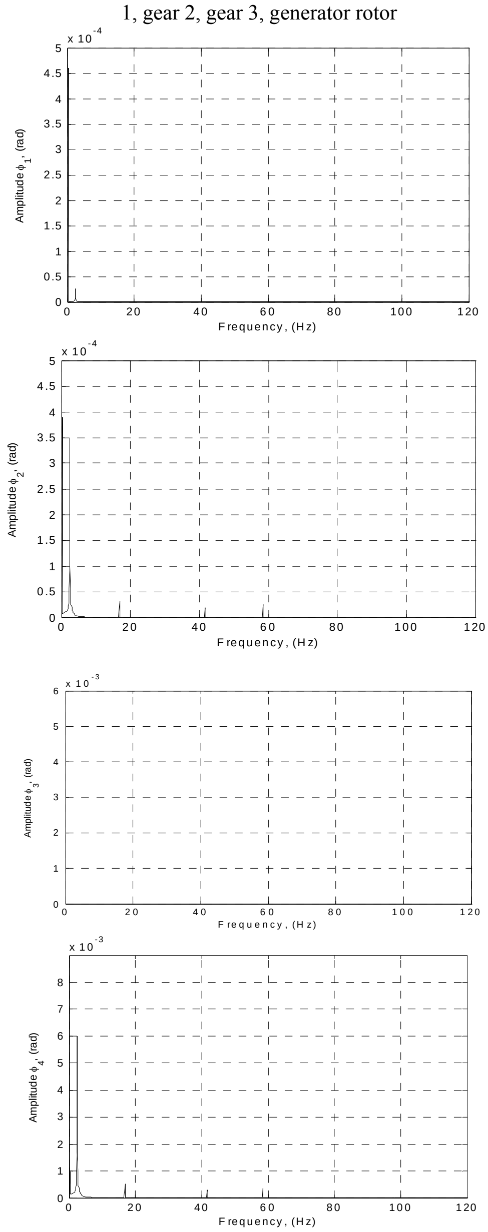

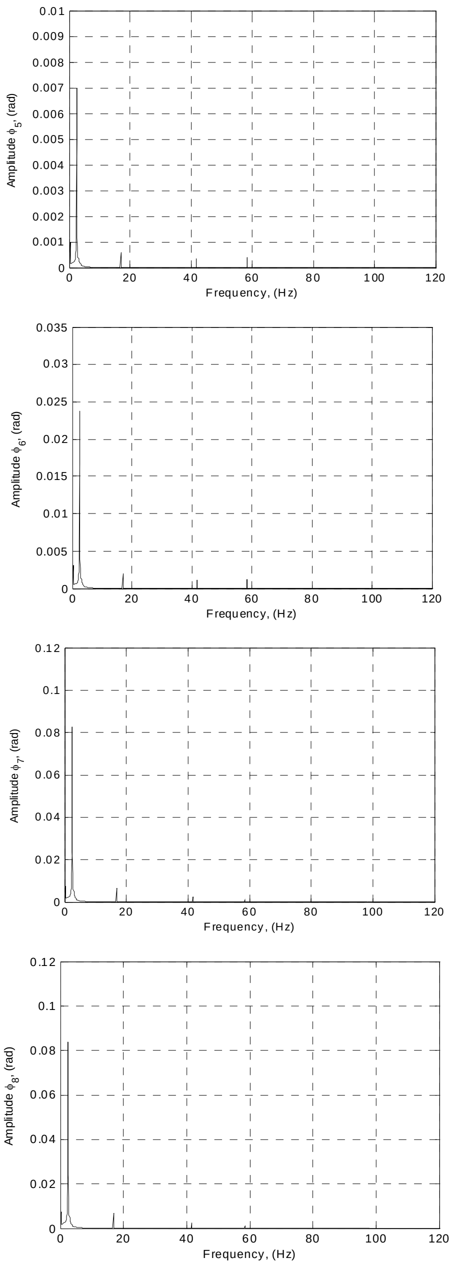

Fig. 7. Amplitude-frequency characteristics. From top: Rotor (hub), carrier, planets, sun, gear 1, gear 2, gear 3, generator rotor

VI. CONCLUSIONS AND FUTURE RESEARCHES

The purpose of this article is to develop a detailed multi-body model of the wind turbine with complex drive train. The starting point in the research of torsional vibrations is finding the natural frequencies and mode shapes, which indicate the frequency range of interest.

The time series and amplitude-frequency characteristics of absolute rotation angles of drive train parts are presented. For presented wind turbine only the natural frequency 2.51 Hz is in the frequency range of external disturbances and for this reason the top amplitudes have this frequency. This frequency is the rotational speed of hub. The amplitudes with frequencies of the generator disturbance harmonics 16.8, 41.6 and 58.4 Hz are less, since they are out of the range of natural frequencies.

The results confirm the presence of vastly dynamic loads in the gearbox parts.

Future researches are planed to extend the current model and to add the effects of bearing flexibilities and gearbox suspension.

Finally, it is important to validate and improve the wind turbine dynamic model by obtaining experimental measurements.

REFERENCES

[1] А. Важнов, *Переходные процессы в машинах переменного тока*, Ленинград, Энергия, 1980.

[2] В. Вейц, А. Кочура, А. Мартыненко, *Динамические расчеты приводов машин*, Москва, Машиностроение,1971.

[3] В. Вейц, М. Коловский, А. Кочура, *Динамика управляемых машинных агрегатов*, Москва, Наука,1984.

[4] Н. Минчев, В. Григоров, *Вибродиагностика на ротационни и бутални машини*, София, ДИ-Техника, 1998.

[5] A. Ahlström, "Aeroelastic Simulation of Wind Turbine Dynamics," Royal Institute of Technology, Stockholm, April 2005.

[6] V. Ambarisha, R. Parker, "Suppression of Planet Mode Response in Planet Gear Dynamics Through Mesh Phasing," – J. Vibration and Acoustics, 2006, vol.128, pp.133-142.

[7] F. Amirouche, *Fundamentals of Multibody Dynamics – Theory and Applications*, Birkhäuser, Boston, 2006.

[8] A. Andersson, L. Vedmar, "A Dynamic Model to Determine Vibrations in Involute Helical Gears," J. Sound and Vibrations, 260, pp.195-212, 2003.

[9] T. Burton, D. Sharpe, N. Jenkins, E. Bossanyi, *Wind Energy Handbook*, Chichester, John Wiley & Sons, 2001.

[10] M. Coutinho, *Dynamic Simulations of Multibody Systems*, New-York, Springer-Verlag, 2001.

[11] Deutsches Institut für Normung, *Calculation of Load Capacity of Cylindrical gears*, DIN 3990, 1987.

[12] J. Ekanayake, L. Holdsworth, N Jenkins, "Comparison of 5th Order and 3rd Order Machine Models for Doubly Fed Induction Generator (DFIG) Wind Turbines," Electric Power Systems Research, vol.67, pp.207-215, 2003.

[13] T. Fuglseth, "Modelling a 2.5 MW direct driven wind turbine with permanent magnet generator," Smøla, 5-11 June 2005.

[14] P. Gold et al, "Simulation of The Three-Dimensional Vibration Behavior of a Wind Energy Plant," SIMPACK Users Meeting 2004, Wartburg-Eisenach, 09-10.11.2004.

[15] M. Hand, M. Balas, "Blade Load Mitigation Control Design for a Wind Turbine Operating in the Path of Vortices", Wind Energy, John Wiley & Sons, 2007.

[16] M. Hansen, *Aerodynamics of Wind Turbines*, Earthscan Publications Ltd., 2001.

[17] A. Hansen, P. Sørensen, F. Blaabjerg, J. Becho, "Dynamic modelling of wind farm grid interaction," Wind Engineering, Vol. 26, No.4, pp.191-208, 2002.

[18] A. Heege, "Computation of Dynamic Loads in Wind Turbine Power Trains – DEWI Magazin," Nr.23, August 2003.

[19] A. Heege, J. Bertran, Y. Radovcic, "Fatigue Load Computation of Wind Turbine Gearboxes by Coupled Finite Element, Multi-Body System and Aerodynamic Analysis," Wind Energy, John Wiley & Sons, 2007.

[20] H. Jordan, V. Klíma, P. Kovacs, *Asynchronmaschinen: Funktion, Theorie, Technishes*, Budapest, Akadémia Kiadó, 1975.

[21] A. Kahraman, "Effect of Axial Vibrations on the dynamics of a helical gear pair," J. Vibration and Acoustics, 115, pp.33-39, 1993.

[22] P. Kovacs, *Transient Phenomena in Electrical Machines*, Elsevier Science Publishers B.V., 1984.

[23] J. Leishman, T. Beddoes, "A Semi-Empirical Model for Dynamic Stall, Journal of The American Helicopter Society," Washington, Jun 1986.

[24] J. Leishman, *Principles of Helicopter Aerodynamics*, Cambridge University Press, 2000.

[25] G. Litak, M. Friswell, "Dynamics of a Gear System with Faults in Meshing Stiffness," Kluwer Academic Publishers, 2004.

[26] O. Lundvall, N. Strömberg, A. Klarbring, "A Flexible multi-body Approach for Frictional Contact in Spur Gears," J. Sound and Vibrations, 278, pp.479-499, 2004,.

[27] P. Nikravesh, *Computer-Aided Analysis of Mechanical Systems*, New Jersey, Prentice Hall, 1988.

[28] A. Parey, M. Badaoui, F. Guillet, N. Tandon, "Dynamic Modelling of Spur Gear Pair and Application of Empirical Mode Decomposition – Based Statistical Analysis for Early Detection of Localized Tooth Defect," J. Sound and Vibrations, 294, pp.547-561, 2006.

[29] J. Peeters, D. Vandepitte, P. Sas, S. Lammens, "Comparison of analysis techniques for the dynamic behaviour of an integrated drive train in a wind turbine," Proc. of ISMA, vol.III, pp.1397-1405, 2002.

[30] J. Peeters, D. Vandepitte, P. Sas, "Analysis of Internal Train Dynamics in a Wind Turbine," Wind Energy, vol.9, pp.141-161, 2006.

[31] J. Peeters, D. Vandepitte, P. Sas, "Flexible multibody model of a three-stage planetary gearbox in a wind turbine," Proc. ISMA, pp.3923-3941, 2004.

[32] J. Peeters, "Simulation of Dynamic Drive Train Loads in a Wind Turbine," Katholieke Universiteit Leuven, Juni 2006.

[33] K, Pierce, "Wind Turbine Load Prediction Using the Beddoes-Leishman Model for Unsteady Aerodynamics and Dynamic Stall," The University of Utah, August 1996.

[34] B. Rabelo, W. Hofman, M. Tilscher, A. Basteck, "A New Topology for High Powered Wind Energy Converters," EPE-PEMC'2004.

[35] G. Ramtharan, N. Jenkins, O. Anaya-Lara, E. Bossanyi, "Influence of Rotor Structural Dynamics Representations on the Electrical Transient Performance of FSIG and DFIG Wind Turbines," Wind Energy, John Wiley & Sons, 2007.

[36] P. Rosas, "Dynamic Influences of Wind Power on the Power System," Ørsted, March 2003.

[37] A. Shabana, *Dynamics of Multibody Systems*, New York, Cambridge University Press, 2005.

[38] L. Shi, Z. Hu, J. Hao, Y. Ni, "Modelling Analysis of Transient Stability Simulation with High Peneration of Grid-connected Wind Farms of DFIG Type," Wind Energy, John Wiley & Sons, 2007.

[39] B. Shlecht, T. Shulze, "Simulation of Drive trains in Wind Turbine with SIMPACK" SIMPACK Users Meeting 2003, Freiburg im Breisgau, 08-09.04.2003.

[40] B. Shlecht, T. Shulze, T. Hähnel, "Multibody-System-Simulation of Wind Turbines for Determination of Additional Dynamic Loads," SIMPACK Users Meeting 2004, Wartburg-Eisenach, 09-10.11.2004.

[41] B. Shlecht, T. Shulze, T. Rosenlocher, "Simulation of Heavy Drive Trains with Multimegawatt Transmission Power in SimPACK," SIMPACK Users Meeting 2006, Kurhaus in Baden-Baden, 21-22.03.2006.

[42] P. Sørensen et al., "Simulation and Verification of Transient Events in Large Wind Power Installations," Rizø National Laboratory, Roskilde, October 2003.

[43] P. Sørensen, A. Hansen, T. Lund, H Binder, "Reduced Models of Doubly Fed Induction Generator System for Wind Turbine Simulations," Wind Energy, vol.9, pp.299-311, 2006.

[44] K. Thomsen, P. Sørensen, A. Hansen, "Generator Dynamics in Aeroelastic Analysis and Simulations," Rizø National Laboratory, Roskilde, May 2003.

[45] M. Todorov, G. Vukov, I. Dobrev, "A Dynamic Multibody Model for Determination of the Torsional Vibration of the Wind Turbine," J. Механика на машините, v.2, pp.32-35, 2007.

[46] L. Vedmar, A. Andersson, "A Method to Determine Dynamic Loads on Spur Gear Teeth and on Bearings," J. Sound and Vibrations, 267, pp.1065-1084, 2003.

[47] H. Vinayak, R. Singh, "Multi-Body Dynamics and Modal Analysis of Compliant Gear Bodies," J. Sound and Vibrations, 210(2), pp.171-214, 1998.

[48] VOITH, "WinDrive®-A New Drive Train Concept for Wind Turbine," SIMPACK Users Meeting 2006, Kurhaus in Baden-Baden, 21-22.03.2006.

[49] J. Wittenburg, *Dynamics of Systems of Rigid Bodies*, Stuttgard, B.G. Teubner 1977.

[50] J. Wojnarowski, V. Onishchenko, "Tooth Wear Effect on Spur Gear Dynamics," Mechanics and Machine Theory, 38, pp.161-178, 2003.

[51] C. Yuksel, A. Kahraman, "Dynamic Tooth Loads of Planetary Gear Sets Having Tooth Profile Wear," Mechanics and Machine Theory, 39, pp.695-715, 2004.

[52] J. Zakrajesek, "Comparison of Gear Dynamics Computer Programs at NASA Lewis Research Centre," NASA Technical Paper 2901, 1989.